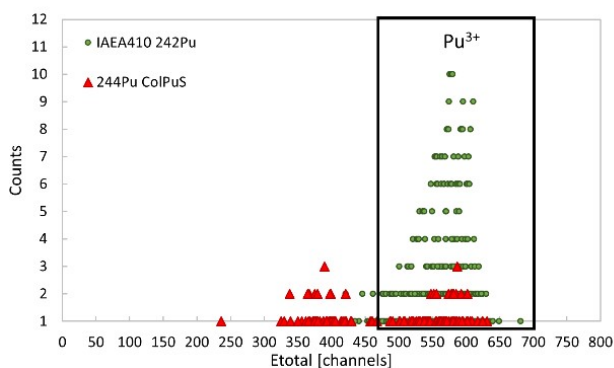
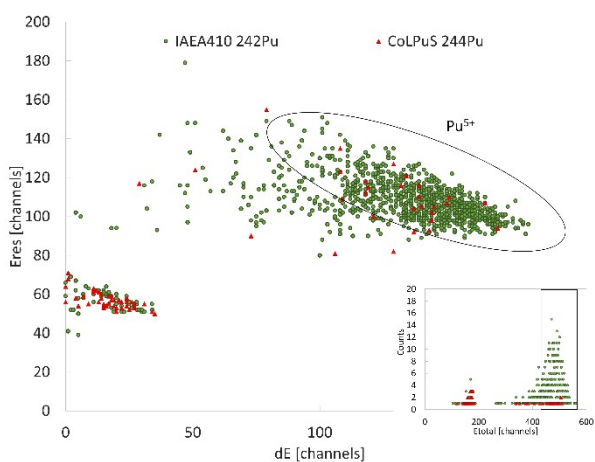


Supplementary Fig. 1 Total energy loss spectrum, obtained from GIC of the 1MV AMS system, for 2.53 MeV $^{242}\text{Pu}^{5+}$ (for IAEA 410 sediment sample, green circles) and $^{244}\text{Pu}^{5+}$ ions (for ColPuS Pu standard, red triangles). The isotopes are used to set the region of interest



Supplementary Fig. 2 Two dimensional Eres – dE and Total energy (minimized) spectrums, obtained from GIC of the 3MV AMS system, for 14.37 MeV $^{242}\text{Pu}^{5+}$ (for IAEA 410 sediment sample) and $^{244}\text{Pu}^{5+}$ ions (for ColPuS Pu standard)



Supplementary Table 1 Radiochemical recoveries of Pu (ED – Electrodeposition, MP – Microprecipitation)

Sample	Measurement time	Measured Activity [Bq]	Chemical yield [%]
AS2 ED, only ^{242}Pu	6.9h	0.016 ± 0.003	76.6
AS7 MP, only ^{242}Pu	6.9h	0.021 ± 0.004	94.9
AS10 MP, IAEA 410 spiked with ^{242}Pu and TEVA separation	30.3h	0.018 ± 0.001	85.7
AS16 MP, only ^{242}Pu and TEVA separation	6.9h	0.054 ± 0.006	94.3

Supplementary Table 2 The isotopic ratios for $^{244}\text{Pu}/^{239}\text{Pu}$ with 2σ uncertainties (using the confidence level given in ^[1]) and $^{240}\text{Pu}/^{239}\text{Pu}$ with 1σ uncertainties

Sample/ Code	$^{244}\text{Pu}/^{239}\text{Pu} (\cdot 10^{-4})$	$^{240}\text{Pu}/^{239}\text{Pu}$
IAEA 410.1 IFIN-HH, this work	3.38 ± 0.65	0.250 ± 0.024
IAEA 410.2 IFIN-HH, this work	$3.42 \begin{smallmatrix} +1.87 \\ -1.36 \end{smallmatrix}$	0.265 ± 0.026
IAEA 410.3 IFIN-HH, this work	4.98 ± 0.98	0.259 ± 0.024
IAEA 410.4 IFIN-HH, this work	$4.50 \begin{smallmatrix} +2.79 \\ -2.02 \end{smallmatrix}$	0.218 ± 0.023
IAEA 410.5 IFIN-HH, this work	$2.50 \begin{smallmatrix} +1.89 \\ -1.33 \end{smallmatrix}$	0.226 ± 0.022
IAEA 410.6 IFIN-HH, this work	$3.38 \begin{smallmatrix} +2.29 \\ -1.63 \end{smallmatrix}$	0.290 ± 0.069
IAEA 410.7 IFIN-HH, this work	$1.97 \begin{smallmatrix} +1.91 \\ -1.24 \end{smallmatrix}$	0.265 ± 0.064
Bikini Atoll, Island, BL5 ^[2]	$3.1 \begin{smallmatrix} +5.4 \\ -2.0 \end{smallmatrix}$	0.319 ± 0.026
Bikini Atoll, Island, BL6 ^[2]	5.4 ± 1.6	0.323 ± 0.011
IAEA 410, CNA Seville, Spain ^[3]	/	0.257 ± 0.023
IAEA 412.1 IFIN-HH, this work	$1.22 \begin{smallmatrix} +1.11 \\ -0.77 \end{smallmatrix}$	0.194 ± 0.021
IAEA 412.2 IFIN-HH, this work	$1.34 \begin{smallmatrix} +1.22 \\ -0.85 \end{smallmatrix}$	0.191 ± 0.018
IAEA 412.3 IFIN-HH, this work	$2.65 \begin{smallmatrix} +1.69 \\ -1.17 \end{smallmatrix}$	0.156 ± 0.016
IAEA 412.4 IFIN-HH, this work	$1.23 \begin{smallmatrix} +1.20 \\ -0.78 \end{smallmatrix}$	0.168 ± 0.017
IAEA 412, CNA Seville, Spain ^[3]	/	0.182 ± 0.015
Pacific Ocean, deep-sea manganese crust ^[4]	1.0 ± 0.3	/

References

1. G. J. Feldman, R. D. Cousins, Phys. Rev., 1998, Volume D 57, 3873, <https://doi.org/10.1103/PhysRevD.57.3873>
2. J. Lachner, M. Christl, T. Bisinger, R. Michel, H.-A. Synal, Applied Radiation and Isotopes, 2010 Volume 68, Pages 979-983, <https://doi.org/10.1016/j.apradiso.2010.01.043>
3. E. Chamizo, M. López-Lora, M. Villa, N. Casacuberta, J. M. López-Gutiérrez, M. Khanh Pham, Nucl. Instr. Meth. B, 2015, Volume 361, Pages 535-540, <http://dx.doi.org/10.1016/j.nimb.2015.02.066>
4. A. Wallner, T. Faestermann, J. Feige, C. Feldstein, K. Knie, G. Korschinek, W. Kutschera, A. Ofan, M. Paul, F. Quinto, G. Rugel., P. Steier, Nature Communications, 2015, Volume 6, 5956, <https://doi.org/10.1038/ncomms6956>